COMPDYN 2011
III ECCOMAS Thematic Conference on
Computational Methods in Structural Dynamics and Earthquake Engineering
M. Papadrakakis, M. Fragiadakis, V. Plevris (eds.)
Corfu, Greece, 25–28 May 2011

IN-PLANE DESIGN LOADS FOR SEISMIC ASSESSMENT AND RETROFIT OF WALLS IN UNREINFORCED MASONRY BUILDINGS

Jason M. Ingham[1], Charlotte L. Knox[2], Aaron W. Wilson[3], and Kenneth J. Elwood[4]

[1] Department of Civil and Environmental Engineering, The University of Auckland
Private Bag 92019, Auckland, New Zealand
e-mail: j.ingham@auckland.ac.nz

[2] Department of Civil and Environmental Engineering, The University of Auckland
Private Bag 92019, Auckland, New Zealand
Ckno015@aucklanduni.ac.nz

[3] Department of Civil and Environmental Engineering, The University of Auckland
Private Bag 92019, Auckland, New Zealand
Awil222@aucklanduni.ac.nz

[4] Department of Civil Engineering, University of British Columbia
6250 Applied Science Lane, Vancouver, BC, V6T 1Z4, Canada
elwood@civil.ubc.ca

Keywords: Unreinforced masonry, Flexible diaphragms, Seismic Loads, Design guide.

Abstract. *It is well established and routinely observed that unreinforced masonry buildings perform poorly in large earthquakes. This knowledge directly points to the need for a detailed procedure for the seismic assessment and retrofit of unreinforced masonry buildings. Pivotal to the entire assessment and retrofit process is the accurate treatment of the dynamic characteristics of flexible timber floor diaphragms, and the development of a straightforward and accurate method for determining the in-plane seismic loads on walls when accounting for both excitation due to self weight, and seismic demand transmitted via wall-diaphragm connections.*

Pertinent details of the M7.1 2010 Darfield (Canterbury) earthquake are presented, followed by a review of results from a large scale experimental program that investigated the strength and stiffness characteristics of timber diaphragms. Next, details are provided of a procedure for determining diaphragm dynamic characteristics recognizing that diaphragm deformations are primarily associated with shear rather than flexure. Finally, details are summarised of a methodology now adopted in New Zealand for determining the in-plane seismic demand on unreinforced masonry walls.

1 INTRODUCTION

Unreinforced masonry (URM) buildings represent the predominant architectural heritage of many nations, and outside of Europe were typically constructed with solid clay brick perimeter walls and comparatively flexible timber floor diaphragms. Unfortunately the preservation of these buildings in seismically active regions is threatened due to their well established inadequacy to withstand earthquakes, as recently demonstrated again in the 2010 Darfield earthquake, which was the largest natural disaster to occur in New Zealand since the 1931 Hawke's Bay earthquake. Observed damage in the earthquake included toppled chimneys and parapets, failure of gables and poorly secured face-loaded walls, and in-plane damage to masonry frames.

Timber floor diaphragms are widely recognized to have significant impact on the overall seismic response of URM structures, and the accurate assessment of diaphragms is therefore crucial during the seismic assessment and retrofit of URM buildings. A series of full-scale diaphragm tests that were performed to generate data to aid in understanding the dynamic characteristic of flexible timber diaphragms is presented.

When compared to the URM buildings of most countries worldwide, the URM building stock in New Zealand is comparatively homogeneous in terms of age, material properties, and architectural form. This observation presents an opportunity to develop a detailed seismic assessment guideline for these buildings that has the dual goals of providing clarification on the appropriate method for deploying existing recommendations, plus incorporating new research results to arrive at the most accurate assessment of seismic capacity currently possible. Such an exercise allows the seismic strength of the URM building to then be expressed in terms of the 'percentage of New Building Strength' (%NBS) and to establish whether seismic improvement of the building is necessary.

2 OVERVIEW OF THE 2010 DARFIELD EARTHQUAKE

2.1 Introduction

At 4.35 am on the morning of Saturday the 4th of September 2010 a magnitude 7.1 earthquake occurred approximately 40 km west of the city of Christchurch NZ at a depth of about 10 km [1], having an epicentre located near the town of Darfield. The ground motion had a peak ground acceleration of about 0.25g and a spectral acceleration in the plateau region of about 0.75g, which corresponds well with the design spectra for a site class D soil site in Christchurch for spectral periods greater than 0.2 seconds. In general, the earthquake represented 67-100% of the design level event, depending upon the spectral period being considered (see Figure 1), with most of Canterbury reporting damage consistent with MM8 on the Modified Mercalli intensity scale. The single most striking statistic was that there were no fatalities directly associated with the earthquake (although there was one heart attack fatality and one person hospitalised due to a falling chimney [2], and the overall impression is that damage in the central business district (CBD) was reasonably contained, restricted primarily to URM buildings and damage to windows in taller steel and concrete structures. The absence of fatalities and more extensive damage was attributed to the comparatively high level of seismic design capability in New Zealand, and the fact that the CBD, which is the region containing the highest density of URM buildings, was almost completely unoccupied at 4.35 am [3].

The soil conditions in Christchurch have three separate material types: river outwash gravels, sands, and marshy ground in former swamp areas, with the central city built mainly on

gravels, although there are pockets of sand and soft soil in former marsh deposits. The earthquake ground motion characteristics shown in Figure 1 reflect the underlying soil condition, with the long period nature of the motion resulting from the soft soils upon which Christchurch is founded. These soft soils effectively act as a filter and remove high frequency ground motion (leading to smaller PGA values than on rock sites) but amplify long period motion, resulting in significantly larger longer period motion at about 2.5 second. As most URM buildings have a fundamental period of 0.2-0.3 seconds, the underlying ground conditions appear to have assisted in reducing the seismic demand in this period range to approximately 70% of the design level loading stipulated in the current New Zealand Loadings Standard. As can be seen in Figure 1(b), strong ground shaking in the CBD had a duration of approximately 30 seconds with similar amplitudes in the two orthogonal recording directions. This lack of distinct directionality probably explains why parapet failures were observed in streets running in both the North-South and East-West directions.

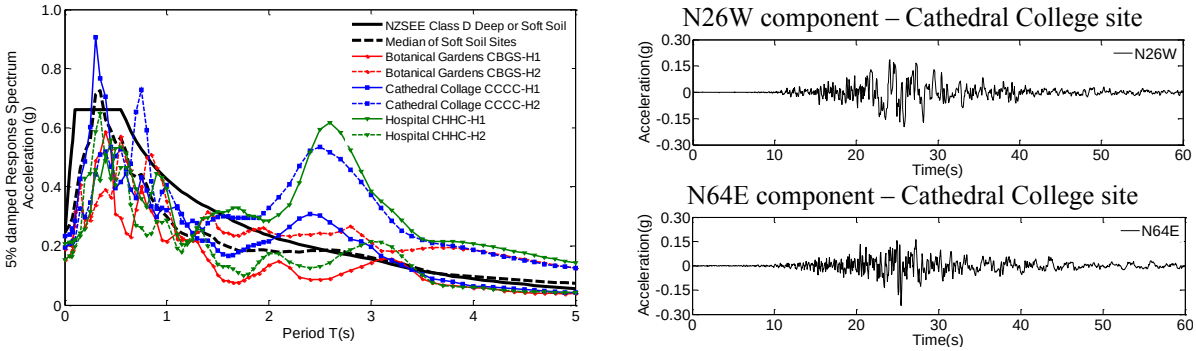

(a) Acceleration spectra (b) Acceleration time-history record

Figure 1: Details of earthquake ground motion [2]

2.2 Building Damage Statistics

In general, the observed damage to URM buildings in the 2010 Darfield Earthquake was consistent with the expected seismic performance of this building form [4]. As part of the emergency response to this earthquake, building were tagging with either a green, yellow or red placard depending, respectively, upon whether a building was safe for public use, had limited accessibility for tenants/occupants, or was not accessible. Many examples of earthquake damage were observed during this exercise, as well as many examples of seismic retrofits to URM buildings that had performed well [5].

2.3 Parapet failures

Numerous parapet failures were observed along both the building frontage and along their side walls, and for several URM buildings located on the corners of intersections, the parapets collapsed on both perpendicular walls (refer Figure 2). Restraint of URM parapets against lateral loads has routinely been implemented since the 1940s, so whilst it is difficult to see these restraints unless roof access is available, it is believed that the majority of parapets that exhibited no damage in the earthquake were provided with suitable lateral restraint. In several cases, it appears that parapets were braced back to the perpendicular parapet, which proved unsuccessful.

2.4 Anchorage failures

Falling parapets typically landed on awnings, resulting in an overloading of the braces that supported these awnings and leading to collapse. Most awning supports in Christchurch involved a tension rod tied back into the building through the front wall of the building. Many of these connections appear to consist of a long, roughly 25 mm diameter rod, with a rectangular steel plate (about 5 mm thick) at the wall end that is about 50 mm wide x 450 mm long and fastened to the rod and positioned either inside the brick wall or in the centre of a masonry pier or wall. In most cases the force on the rod exceeded the capacity of the masonry wall anchorage, causing a punching shear failure in the masonry wall identified by a crater in the masonry (refer Figure 3).

(a) Multiple front wall parapet failures

(b) Corner of Sandyford and Colombo Street

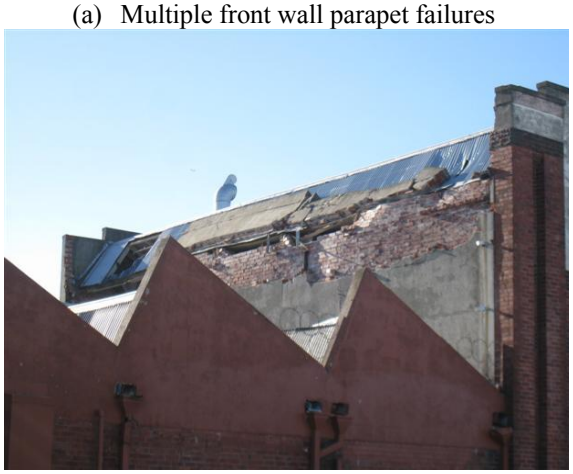

(c) Side wall parapet collapse onto roof.

(d) Corner Columbo and Tuam Street

Figure 2: Examples of typical parapet failures.

2.5 Wall failures

Out-of-plane wall failures were the first images to appear on television directly after the earthquake. Inspection of this damage typically indicated poor or no anchorage of the wall to its supporting timber diaphragm. Several examples of wall failure are shown below. Figure 4(a) shows a corner building that had walls fail in the out-of-plane direction along both directions. Figure 4(b) shows a 3-storey building where walls in the upper two stories suffered out-of-plane failures and Figure 4(c) shows similar damage for a 2-storey building. In all three of these instances, it appears that the walls were not carrying significant vertical gravity loads, other than their self weight, due to the fact that the remaining roof structures appear to

be primarily undamaged. In contrast, Figure 4(d) shows an out-of-plane failure of a side wall which was supporting the roof trusses prior to failure.

3 FLEXIBLE TIMBER DIAPHRAGMS

While URM buildings outside of Europe are typically comprised of rigid clay brick perimeter walls, the floors are usually constructed of comparatively light timber framing. These floors are generally made up of either straight-edge or tongue & groove floorboards nailed perpendicular to joists that span between the URM walls. When perimeter walls are close enough (approximately less than 6 m) joists often span continuously between these elements. For larger spans, joists are typically lapped or butted over intermediate steel or timber cross-beams supported on columns. Diaphragm blocking and chord elements are almost never present, and timber cross-bracing is typically fitted intermittently between joists to prevent out-of-plane buckling. Joist ends are typically either simply supported on a brick ledge resulting from the perimeter walls reducing in width at each storey height, or pocketed into the wall to a depth equal to one brick width. Examples of timber floor configurations are given in Figure 5.

(a) Anchorage failure (b) Close-up of failed anchorage detail

Figure 3: Anchorage failure of awning brace due to parapet collapse.

Timber floors in URM buildings act as diaphragms that have routinely demonstrated significant influence on the seismic performance of the complete URM structure due to their flexible nature and often inadequate connection to the perimeter URM walls [6] (Bruneau 1994). The in-plane strength and stiffness of these diaphragms is therefore crucial to the overall performance of the URM building and accurate assessment of their performance is essential for the design of appropriate retrofitting techniques when seismic strengthening is required. Due to a complete lack of experimental data and appropriate analysis [7-9], the validity of diaphragm assessment procedures offered in current state-of-the-art assessment documents [10-11] are questionable. Furthermore, communication from engineering practitioners suggests that such documents are difficult to understand and to follow with confidence. Given these shortcomings, significant motivation currently exists to investigate the performance of timber floor diaphragms and the accuracy of assessment procedures. Before non-destructive testing techniques are considered as a viable assessment tool, it is necessary to generate in-plane performance data for timber diaphragms with which to appropriately update and improve current seismic assessment desktop procedures.

Results of a series of full-scale diaphragm tests are summarized and are used to review the validity of the current desktop assessment procedures published in [10] and [11]. Performance

predictions using the assessment techniques are compared against experimental results and where possible, recommendations to improve their accuracy are suggested.

3.1 As-built diaphragm testing

A total of four diaphragm specimens labeled FS1a to FS4a, constructed with new pine timber, were tested. Each specimen measured 10.4 m x 5.535 m and was comprised of 135 mm x 18 mm straight edge floorboards nailed perpendicular to 45 mm x 290 mm joists spaced at 400 mm centers. Joists were orientated in the 5.535 m dimension. Cross-bracing was fitted between the joists at 1/3 joist length locations using 45 mm x 75 mm framing. Every floorboard-joist connection was fastened using two 75 mm x 3.15 mm bright power driven nails spaced at approximately 95 mm.

(a) Corner Worcester and Manchester streets

(b) 118 Manchester Street

(c) 179 Victoria Street

(d)

Figure 4: Examples of out-of-plane failures in solid masonry walls.

Diaphragms FS1a and FS2a were tested in the direction parallel to joists so that the diaphragm span to depth ratio was 1.88 to 1. In this direction the two side joists were bolted to steel frames that were fastened to the warehouse concrete slab which replicated in-situ boundary conditions where the edge joists would simply be bolted intermittently to the perimeter URM walls (see Figure 6(a)). Lateral loading was introduced into the diaphragm using a hinged steel frame 'whiffle tree' on castors that distributed the hydraulic actuator point load into four equal point loads. It can be observed in Figure 6(b) that the loading frame was comprised of a main truss and two secondary beams that were capable of rotating with the deforming diaphragm. Reversed cyclic loading was achieved by positioning loaders on both ends of the loaded joists, and post-tensioning these loaders together using M16 threaded rods that spanned the depth of the diaphragm (Figure 6(b)). The diaphragm was supported verti-

cally by Teflon pads that allowed the diaphragm to deform laterally without measurable friction. Diaphragm FS1a shown in Figure 6(a) was a homogenous diaphragm while diaphragm FS2a shown in Figure 6(c) included a corner penetration measuring 3.2 m x 1.08 m that represented a typical stairwell present in many timber diaphragms.

Diaphragms FS3a and FS4a were tested in the direction perpendicular to joists so that the diaphragm span to depth ratio was 1 to 1.88. Realistic conditions were created for this set-up by constructing URM walls on each side of the diaphragm for the joists to pocket into, similar to that illustrated in Figure 5(b). Sliding of the brick walls was prevented by post-tensioning the walls with M16 rods epoxied into the warehouse concrete slab (measurement of wall position during testing showed that no wall displacement was observed). Loading was introduced into the diaphragm using the same hinged steel frame as for the previous set-up but with only two points of loading. Diaphragms FS3a and FS4a were equivalent in construction except that diaphragm FS3a had continuous joists spanning between the brick walls while diaphragm FS4a had discontinuous joists with a two-bolt lapped central connection.

(a) Underside showing joists, sheathing and cross-bracing

(b) Joists pocketed into URM perimeter wall

Figure 5: Typical timber diaphragm configuration

3.2 Test Results

Overall the diaphragms displayed flexible and highly nonlinear characteristics with low levels of hysteretic pinching, as illustrated in the force versus midspan displacement plots in Figure 7. The open hysteretic loops demonstrate that these diaphragms are capable of dissipating considerable amounts of energy when subject to lateral loading. No splitting of timber, nail tear-out or other failure mechanisms were observed during testing, even at displacements in excess of 150 mm, and all diaphragms appeared to remain completely serviceable at the conclusion of each test.

A comparison of the force-displacement responses of specimens FS2a and FS1a suggests that a small diaphragm opening such as a stairwell does not significantly affect the diaphragm's performance, with these responses being largely indistinguishable. It is appreciated that larger penetrations may worsen this effect however. Another interesting observation is that diaphragms FS3a and FS4a behaved analogously despite the presence of a central discontinuity in the joists in diaphragm FS4a. This could be explained by the deformation profile of the diaphragms displaying little amounts of relative displacement between the two point-load locations. With the majority of deformation occurring in the outer regions of the diaphragm, the curvature near the centralized joist connection was low and therefore considerably reduced its effect on diaphragm response.

(a) Diaphragm FS1a

(b) Loading frame set-up

(c) Penetration in Diaphragm FS2a

(d) Diaphragm FS3a/4a

Figure 6: Experimental program

It is difficult to directly compare force-displacement response between the two principal loading directions due to the influence of diaphragm geometry. Diaphragms FS3a and FS4a demonstrated greater stiffness and strength than FS1a and FS2a, but this is clearly due to a considerably lower span to depth ratio. As a general observation, the hysteretic loops are larger in the direction parallel to joists which could result from greater engagement of the yielding nail couples in this direction as opposed to loading in the direction perpendicular to joists, where the nail couples are less engaged and the out-of-plane bending of the joists has greater influence on response.

Figure 8 shows the bilinear curves produced for diaphragm tests FS1a to FS4a. The bilinear curves defined the yield force (F_y), yield displacement (Δ_y), maximum force at Δ = 150 mm (F_{max}), and initial and secondary stiffness (K_1 and K_2) values presented in Table 2 that were used to calculate the desired diaphragm performance parameters. Diaphragm stiffness K_d was defined as initial stiffness K_1 while shear strength R_n was calculated by simply dividing yield force by two times the diaphragm depth. Ductility was determined using the conventional assumption of elastic-perfectly plastic response and calculating the ratio between maximum displacement and yield displacement. These values are presented in Table 1 for comparison.

	Shear strength, R_n [kN/m]				***Stiffness K_d*** [kN/m]			***Shear stiffness, G_d*** [kN/m]			***Ductility, μ***		
	NZSEE (i)	NZSEE (ii)	ASCE	Exp	NZSEE	ASCE	Exp	NZSEE	ASCE	Exp	NZSEE	ASCE	Exp
FS1a	1.4	6.0	1.75	1.6	207	745	647	97	350	304	-	2.0	5.6
FS2a	1.4	6.0	1.75	1.6	207	745	606	97	350	284	-	2.0	5.2
FS3a	1.4	6.0	1.75	1.2	730	2630	1297	97	350	173	-	2.0	7.7
FS4a	1.4	6.0	1.75	1.2	730	2630	1842	97	350	245	-	2.0	10.8

Table 1: Diaphragm performance parameters

	F_y [kN]	Δ_y [mm]	F_{max} [kN]	Δ_{max} [mm]	K_1 [kN/m]	K_2 [kN/m]
FS1a	17.2	26.6	36.8	150	647	159
FS2a	17.6	29.1	35.9	150	606	151
FS3a	25.4	19.6	110.0	150	1297	649
FS4a	25.7	13.9	104.3	150	1842	578

Table 2: Experimental bilinear values

3.3 Discussion

Overall, the guidelines offered in both assessment documents poorly predict diaphragm performance. The values listed in Table 1 illustrate that diaphragm shear strength, stiffness, shear stiffness and ductility are either under predicted or over predicted using the NZSEE [10] and ASCE 41-06 [11] assessment procedures. Shear strength is the most accurately predicted parameter with approximately 10% discrepancy from experimentally determined values, with the exception of the alternative default value offered by NZSEE that grossly over estimates strength. The reason for this large discrepancy remains unknown. Diaphragm stiffness and shear stiffness is considerably under predicted using the methodology in NZSEE, while is over predicted using ASCE 41-06 guidelines. NZSEE offers no explicit guidance for diaphragm ductility while ASCE 41-06 provisions where shown to under estimate diaphragm ductility by up to five times.

An important observation from the experimental performance parameters listed in Table 1 is the highly orthotropic behavior demonstrated by the timber diaphragms. The shear strength and shear stiffness values, which are independent of diaphragm geometry, are significantly different in each principal direction of the diaphragm, yet the current assessment documents offer no provisions to address this behavior. In order to improve the transparency and accuracy of the assessment procedures, diaphragm performance parameters should be explicitly provided for in each principal direction.

It is recognized that heritage diaphragm performance may differ from the experimental performance values presented in Table 1 due to out-dated construction materials and the effects of age and decay. A component of the current research program involves testing extracted floor sections and nail connections from ~100 year old timber floor diaphragms. It is hoped that the data generated from testing will provide the necessary information to appropriately modify the performance parameters to ensure they are representative for heritage con-

struction. For the interim, the considerable difference observed between predicted and measured diaphragm performance suggests that the current procedures offered in NZSEE and ASCE 41-06 require updating. In addition, it is believed that these documents should be harmonized so that international assessment procedures are consistent with one another.

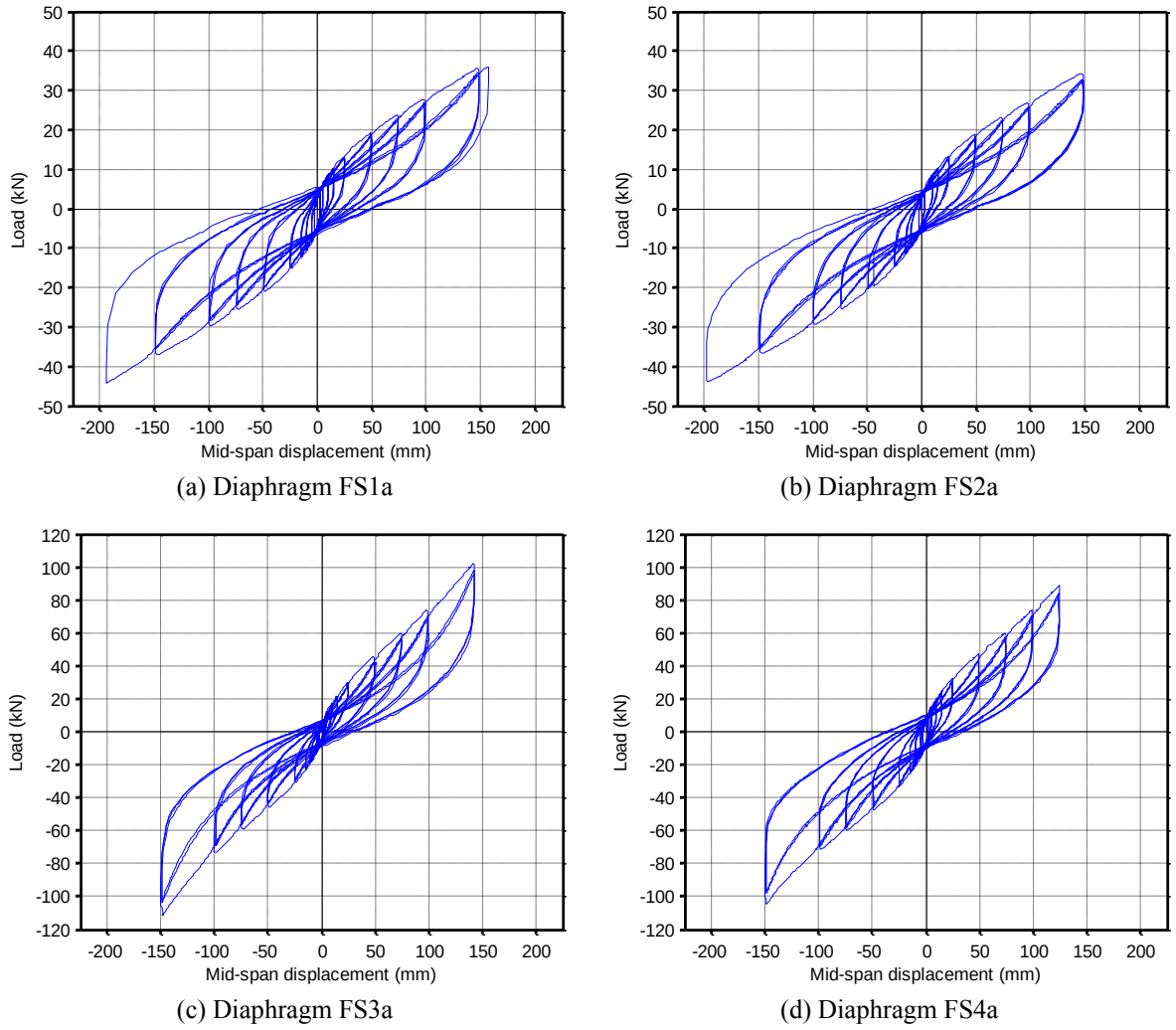

(a) Diaphragm FS1a (b) Diaphragm FS2a

(c) Diaphragm FS3a (d) Diaphragm FS4a

Figure 7: Full-scale diaphragm testing results

4 PERIOD OF FLEXIBLE DIAPHRAGM

Common assessment guides [10, 11] stipulate a diaphragm fundamental period that is calculated as:

$$T = \sqrt{3.07\Delta_d} \tag{1}$$

However neither document clarifies the source of this equation, and as period values derived using Equation 1 can appear somewhat questionable, it is useful to outline the derivation of this equation. If we consider a fixed-ended flexural beam with distributed mass, then the deformed shape and mid-span deflection are as shown in column 1 of Table 3. Note that the period calculation is independent of the magnitude of applied acceleration, but that for convenience it is useful to evaluate deflections when subjected to gravity acceleration, g, even

though horizontal deformations are being considered in the plane of the diaphragm, rather than vertical deflections due to sagging. As outlined in [12], a shape function can be used to describe the beam deformations, which can then be used to develop a generalised mass $m^* = \int_0^L \bar{m}\varphi(x)^2 dx$ and generalised stiffness $k^* = \int EI\varphi''(x)^2\, dx$ (for flexural) or $k^* = \int_0^L \frac{GA}{\kappa}\varphi'(x)^2\, dx$ (for shear). This information can then be introduced to the generalised period equation to obtain a specific expression for the period.

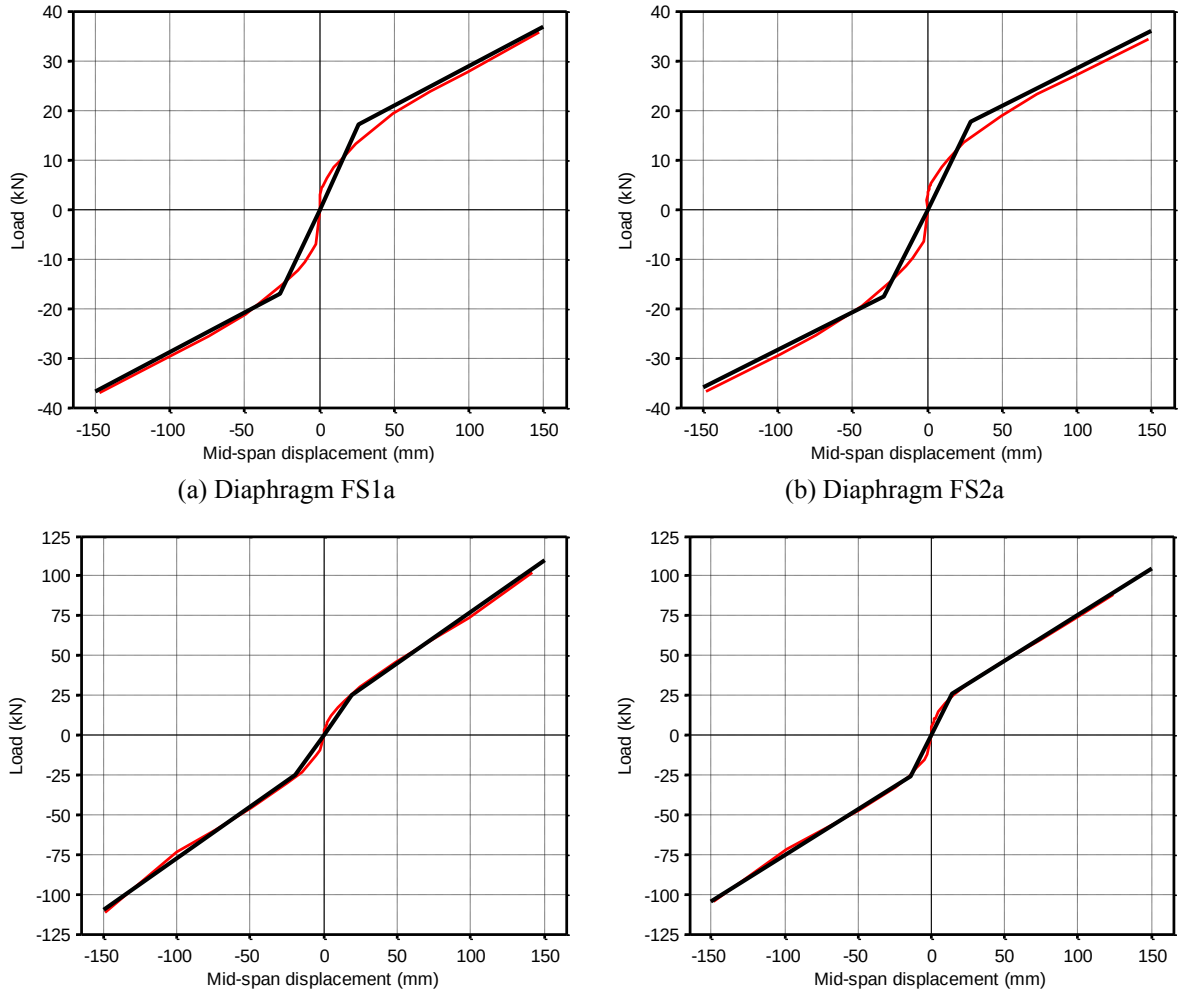

(a) Diaphragm FS1a

(b) Diaphragm FS2a

(c) Diaphragm FS3a

(d) Diaphragm FS4a

Figure 8: Bilinear curves for tested as-built diaphragms

Whilst the above discussion satisfactorily explains the origin of the equation in [10-11], there are several further issues to consider. Firstly, the assumption of the diaphragm having a fixed boundary condition when connected to the in-plane walls is inconsistent with the nature of most diaphragm connection details, and the corresponding period calculations for a pin-ended flexural beam would appear to be more realistic. This information is provided in column 2 of Table 1, illustrating that the boundary effects had an inconsequential influence on the equation coefficient, but a 230% change on the calculated period. More importantly, as flexible diaphragm deformations are governed by shear deformations rather than flexural deformations. Hence the corresponding process is presented in column 3 of Table 3, showing that again this modification has had only a small impact on the coefficient used in the period

	Fixed end flexural beam	Pin ended flexural beam	Shear beam
Deflected geometry, δ(x)	$\delta(x) = \frac{\bar{m}gx^2}{24EI}(L-x)^2$	$\delta(x) = \frac{\bar{m}gx}{24EI}(x^3 - 2Lx^2 + L^3)$	$\delta(x) = \frac{\bar{m}g\kappa}{GA}\left(\frac{L}{2}x - \frac{x^2}{2}\right)$
Maximum deflection	$\Delta_{ff} = \frac{\bar{m}gL^4}{384EI}$	$\Delta_{pf} = \frac{5\bar{m}gL^4}{384EI} = 5\Delta_{ff}$	$\Delta_{sb} = \frac{\bar{m}g\kappa L^2}{8GA}$
Shape function	$\varphi(x) = \frac{16x^2}{L^4}(L-x)^2$	$\varphi(x) = \frac{16x}{5L^4}(x^3 - 2Lx^2 + L^3)$	$\varphi(x) = \frac{8}{L^2}\left(\frac{Lx}{2} - \frac{x^2}{2}\right)$
Generalised mass	$m^* = \frac{256}{630}m$	$m^* = \frac{23808}{47250}m$	$m^* = \frac{8}{15}m$
Generalised stiffness	$k^* = \frac{1024}{5}\frac{EI}{L^3}$	$k^* = \frac{36864}{750}\frac{EI}{L^3}$	$k^* = \frac{16}{3}\frac{GA}{L\kappa}$
General period expression	$T = 2\pi\sqrt{\frac{m^*}{k^*}}$	$T = 2\pi\sqrt{\frac{m^*}{k^*}}$	$T = 2\pi\sqrt{\frac{m^*}{k^*}}$
Specific period expression	$T = \sqrt{3.07\Delta_{ff}}$ $= 1.75\sqrt{\Delta_{ff}}$ $= 1.75\sqrt{\frac{\omega L^4}{384EI}}$ $= 0.0894\sqrt{\frac{\omega L^4}{EI}}$	$T = \sqrt{3.17\Delta_{pf}}$ $= \sqrt{15.85\Delta_{ff}}$ $= 1.78\sqrt{\frac{5\omega L^4}{384EI}}$ $= 0.2032\sqrt{\frac{\omega L^4}{EI}}$	$T = \sqrt{3.21\Delta_{sb}}$ $= 1.79\sqrt{\Delta_{sb}}$ $= 1.79\sqrt{\frac{\omega L^2}{4G_d b}}$ $= 0.8958\sqrt{\frac{\omega L^2}{G_d b}}$

Table 3: Period of flexible diaphragm accounting for boundary effects and deformation modes

calculation. The deflection used in column 3 is consistent with calculated diaphragm deflections according to [11]:

$$\Delta_d = \frac{\bar{m}gL^2}{4G_d b} = \frac{\omega L^2}{4G_d b} \tag{2}$$

In Equation 2 it is important to appreciate that G_d refers to a shear stiffness (having units of kN/m), whereas in the derivation in Table 1, G refers to the Shear Modulus (having units of MPa or kN/m^2). By equating the resulting mid-span deflections and recognising that the shape factor $\kappa = 1.2$ for rectangular sections, we arrive at the relationship:

$$G_d = \frac{2Gt}{\kappa} = \frac{5Gt}{3} = 1.667Gt \tag{3}$$

where *t* is the diaphragm thickness.

5 IN-PLANE LOADS ON SHEAR WALLS

The in-plane loads on shear walls are calculated from two components, one based on the diaphragm response, and the other based on the wall in-plane response. The dynamic response of a multi-storey unreinforced masonry building with flexible diaphragms is concentrated in the diaphragms. The equivalent static method assumes that the in-plane wall is rigid in comparison to the flexible diaphragm for the purpose of calculating the inertial force induced in the diaphragm. Adequate connections between the diaphragm and the in-plane loaded walls are required in order to transfer the inertial force induced in the diaphragms and the out-of-plane loaded walls into the in-plane loaded walls. The wall in-plane response component is based on the shear wall behaving in its fundamental mode. For solid shear walls, calculation of the elastic stiffness and therefore period is relatively simple, but for the case of perforated walls this calculation is much more complicated and hence the recommendation that the in-plane loaded wall period is assumed to lie in the constant acceleration region of the response spectra.

5.1 Damping

Unreinforced masonry does not respond is a classical elastic-plastic manner, exhibiting more of a nonlinear elastic response with pinched hysteretic loops. From analysis of full scale pseudo-static tests on in-plane loaded flanged walls and spandrel/pier sub-structures, a range of 5-15% equivalent hysteretic damping was found. The past recommendation of 15% of critical was formed from a combination of approximately 5% inherent viscous damping associated with elastic structures, 5% hysteretic damping and 5% damping from dynamic impact [10]. The hysteretic damping includes Coulomb (or "dry") damping associated with sliding shear, radiation damping, pinched hysteretic damping associated with flexural/diagonal shear softening and equivalent damping due to impact on rocking. The current recommendation of 5% is supported by the increase in displacement ductility recommended for use in finding demand on in-plane loaded URM shear walls which allows for a reduction in loads based on nonlinear behaviour. The recommendation of 5% of critical is based on the understanding that the increase in ductility to 2, and the reduction due to the structural performance factor, allows for the reduction in load due to nonlinear response and therefore the reduction would be two-fold if damping was also increased.

5.2 Ductility

Unreinforced masonry is generally considered a brittle material and therefore it has been justified in the past to use a displacement ductility factor of 1. The notion of URM as a brittle material is inaccurate and conservative. Ductility is present not from conventional yielding of steel reinforcing bars, but from inelastic response and energy dissipation due to shear sliding along mortar joints and rocking of masonry block elements. When URM walls respond in-plane, particularly with a rocking mechanism, there is significant inelastic displacement capacity and a strongly nonlinear behaviour. A typical shear response is shown in Figure 9(a), and shows no rapid and severe strength loss as associated with a typical brittle failure. The force-displacement plot associated with pier and pier/spandrel sub-structure testing indicates that a flexural failure mechanism, or a flexural/shear combined failure mechanism, is capable of ultimate displacements that greatly exceed the yield displacement, as shown in Figure 9(b). URM buildings have multiple sources of ductility that develop from energy dissipation drawn from shear mechanisms in the in-plane loaded walls, rocking of in-plane loaded URM elements, and energy dissipation from deformations of the timber diaphragms. The recommendation for using a displacement ductility of 2 recognises the nonlinear response of URM walls to

in-plane loading and the energy dissipation that occurs during loading cycles beyond the elastic state.

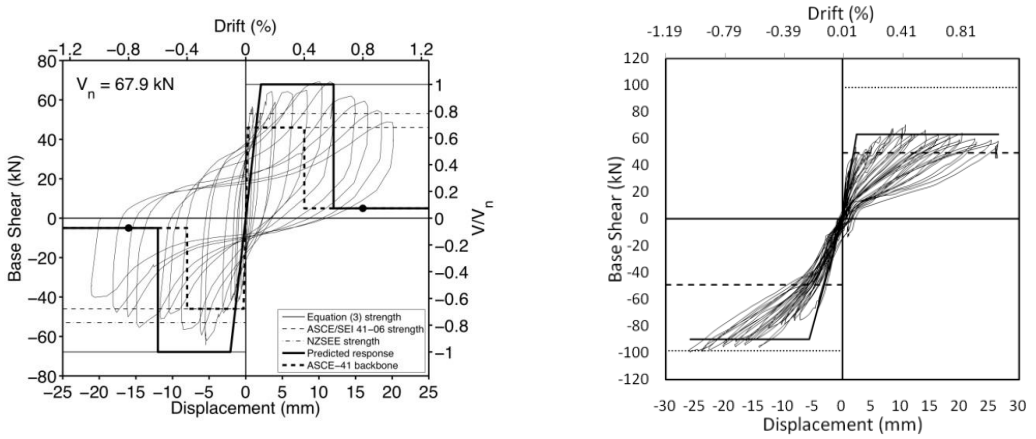

(a) URM pier (b) URM spandrel substructure

Figure 9: Plots of Force-displacement response of URM assemblages

5.3 Vertical Distribution of Inertial Shear Load

A rectangular distribution of the inertial shear load vertically up the height of the building reflects the assumption of effectively rigid wall response in comparison to the flexible diaphragm response. A rectangular distribution implies no modification of the ground accelerations up the height of the wall. Storey shear load is the addition of the diaphragm shear load and the component of in-plane inertial shear load distributed to that level using the Square Root of Sum of Squares rule. Summation of the inertial storey shear load and the individual diaphragm shear loads using a CQC or SRSS method allows for the individual elements to respond at different periods and therefore not necessarily in phase.

6 CONCLUSIONS AND RECOMMENDATIONS

- The significant number of URM buildings damaged in the 2010 Darfield earthquake was consistent with the level of damage that can be expected for an earthquake of this scale.
- The types of failure modes to URM buildings that were observed in the 2010 Darfield earthquake are consistent with those routinely observed in previous last earthquakes.
- Timber floor diaphragms have proven to significantly influence the overall seismic performance of URM buildings.
- Stiffness sand strength data generated from a series of full-scale diaphragm tests will lead to improved accuracy of dynamic modeling of URM buildings.
- Diaphragm deformations are governed by shear deformations rather than flexure deformations.
- In-plane loads on URM walls are comprised of inertial loads and diaphragm transfer loads.

ACKNOWLEDGMENTS

The authors would like to gratefully acknowledge Stuart Oliver of Holmes Consulting Group for his continued guidance, and David Moore of Grayson Engineering and Warwick

Banks of Carter Holt Harvey Woodproducts for their generous support that ensured the successful completion of the flexible diaphragm experimental program reported herein.

REFERENCES

[1] GNS, Darfield earthquake damages Canterbury, http://www.geonet.org.nz/news/article-sep-4-2010-christchurch-earthquake.html, 16 Sept 2010; Retrieved Sept 16, 2010.

[2] NZ Herald, Christchurch earthquake victim: 'I was pinned to the ground', *New Zealand Herald*, http://www.nzherald.co.nz/nz/news/article.cfm?c_id=1&objectid=10673369; Sept 14 2010; Retrieved Sept 20, 2010.

[3] J.M. Ingham, M.C. Griffith, Performance of unreinforced masonry buildings during the 2010 Darfield (Christchurch, NZ) earthquake. *Australian Journal of Structural Engineering*, **In Press**, 2011.

[4] A.P. Russell, J.M. Ingham, Prevalence of New Zealand's Unreinforced Masonry Buildings. *Bulletin of the New Zealand Society for Earthquake Engineering,* **43**(3), 182-201, 2010.

[5] D. Dizhur, N. Ismail, C.L. Knox, R. Lumantarna, J.M. Ingham, Performance of Unreinforced and Retrofitted Masonry Buildings during the 2010 Darfield Earthquake. *Bulletin of the New Zealand Society for Earthquake Engineering,* **43**(4), 321-339, 2010.

[6] M. Bruneau, State-of-the-art report on seismic performance of unreinforced masonry buildings. *Journal of Structural Engineering*, **120**(1), 230-251, 1994.

[7] ABK, *Methodology for mitigation of seismic hazards in existing unreinforced masonry buildings: Diaphragm testing ABK-TR-03*. National Science Foundation, El Segundo, California, 1981.

[8] D.F. Peralta, *Seismic Performance of Rehabilitated Wood Diaphragms*, PhD Dissertation, Texas A&M University, College Station, Texas, 2003.

[9] M. Piazza, *The Role of In-Plane Floor Stiffness in the Seismic Behaviour of Traditional Buildings*. 14th World Conference on Earthquake Engineering, Beijing, China, October 12-17, 2008.

[10] NZSEE, *Assessment and improvement of the structural performance of buildings in earthquakes : prioritisation, initial evaluation, detailed assessment, improvement measures : recommendations of a NZSEE study group on earthquake risk buildings*, New Zealand Society for Earthquake Engineering, Wellington, New Zealand, 2006.

[11] ASCE. *Seismic Rehabilitation of Existing Buildings, ASCE/SEI 41-06*. American Society of Civil Engineers, Reston, VA, 2007.

[12] A.K. Chopra, *Dynamics of Structures (2nd Ed)*, Prentice Hall, Upper Saddle River, NJ, 2001.